Nanoclusters

Deutsche Ausgabe: DOI: 10.1002/ange.201608609
Internationale Ausgabe: DOI: 10.1002/anie.201608609

$[Cu_{13}\{S_2CN^nBu_2\}_6(acetylide)_4]^+$: A Two-Electron Superatom

Kiran Kumarvarma Chakrahari, Jian-Hong Liao, Samia Kahlal, Yu-Chiao Liu, Ming-Hsi Chiang, Jean-Yves Saillard,* and C. W. Liu**

Dedicated to Professor Sunney Chan on the occasion of his 80th birthday

Abstract: *The first structurally characterized copper cluster with a Cu_{13} centered cuboctahedral arrangement, a model of the bulk copper fcc structure, was observed in $[Cu_{13}(S_2CN^nBu_2)_6(C{\equiv}CR)_4](PF_6)$ ($R = C(O)OMe$, C_6H_4F) nanoclusters. Four of the eight triangular faces of the cuboctahedron are capped by acetylide groups in μ_3 fashion, and each of the six square faces is bridged by a dithiolate ligand in μ_2,μ_2 fashion, which leads to a truncated tetrahedron of twelve sulfur atoms. DFT calculations are fully consistent with the description of these Cu_{13} clusters as two-electron superatoms, that is, a $[Cu_{13}]^{11+}$ core passivated by ten monoanionic ligands, with an a_1 HOMO containing two 1S jellium electrons.*

The chemistry of atomically precise noble-metal nanoclusters (NCs) has received significant interest during the last decade owing to their numerous properties and potential use in nanodevices, imaging, medicine, and catalysis.[1,2] Gold and (to a lesser extent) silver NCs of various sizes are well documented. In contrast, comparable copper NCs have remained obscure, in line with the fact that only a very small number of Cu^0 coordination complexes are known to date.[3,4] In our search for silver and copper NCs, we have been able to synthesize several silver mixed-valent species,[5] but thus far, we could only isolate a series of air- and moisture-stable hydrido copper(I) cluster compounds, such as $[Cu_7H(S_2CN^nPr_2)_6]$, $[Cu_8H(S_2CN^nPr_2)_6]^+$, $[Cu_{28}H_{15}(S_2CN^nPr_2)_{12}]^+$, $[Cu_{20}H_{11}\{E_2P(O^iPr)_2\}_9]$ (E = S, Se), and $[Cu_{32}H_{20}\{S_2P(O^iPr)_2\}_{12}]$.[6] Compared with gold and silver, the difficulty associated with the stabilization of copper oxidation states below +I is, at least in part, due to the lower M^I/M^0 half-cell potential of Cu (0.52 V) versus Ag (0.80 V) and Au (1.68 V).[7]

[*] Dr. K. K. Chakrahari, J.-H. Liao, Prof. C. W. Liu
Department of Chemistry, National Dong Hwa University
No. 1, Sec. 2, Da Hsueh Rd., Shoufeng
Hualien 97401 (Taiwan R.O.C.)
E-mail: chenwei@mail.ndhu.edu.tw
Homepage: http://faculty.ndhu.edu.tw/~cwl/index.htm
Dr. S. Kahlal, Prof. J.-Y. Saillard
UMR-CNRS, 6226 "Institut des Sciences Chimiques de Rennes"
University de Rennes 1, 35042 Rennes Cedex (France)
E-mail: jean-yves.saillard@univ-rennes1.fr
Dr. Y.-C. Liu, Dr. M.-H. Chiang
Institute of Chemistry, Academica Sinica
Taipei, 115 (Taiwan R.O.C.)
E-mail: chiangmh@gate.sinica.edu.tw
Supporting information and the ORCID identification number(s) for the author(s) of this article can be found under: http://dx.doi.org/10.1002/anie.201608609.

In fact, the only known copper NC with mixed-valent superatom-like character, namely $[Cu_{25}H_{22}(PPh_3)_{12}]^+$, which has a centered icosahedral $[Cu_{13}]^{11+}$ core, was very recently obtained by Hayton and co-workers[8a] through the reduction of a Cu^I salt in a ligand-deficient environment. A few mixed-metal nanoclusters are also known, namely the 8-electron $[(CuCN^tBu)_4(ZnCp^*)_4]$[8b] and the 18-electron $[Au_{12+n}Cu_{32}(SR)_{30+n}]^{4-}$ series.[8c] Herein, we report the synthesis and characterization of a new copper NC that not only possesses a $[Cu_{13}]^{+11}$ unit but also features a centered dodecahedral (or cuboctahedral) arrangement, an unprecedented configuration in copper cluster chemistry. Moreover, this is the only example of a centered cuboctahedral structure for any discrete tridecanuclear cluster.[9]

The centered icosahedron is the most compact arrangement for a 13-atom unit, and it is very common in transition-metal clusters. For gold and silver, for instance, several examples of clusters containing icosahedral $\{M_{13}\}$ cores have been characterized by single-crystal X-ray diffraction and theoretical computations.[5,10] On the other hand, recent efforts by Zeng et al. have led to the isolation of a couple of fcc-configured NCs, namely $Au_{28}(SPh\text{-}t\text{-}Bu)_{20}$ and $Au_{36}(SPh\text{-}t\text{-}Bu)_{24}$.[11,12] These findings oppose the previous idea that non-fcc configurations would be more stable than fcc-linked cuboctahedral configurations.[13] Nevertheless, discrete centered dodecahedral $\{M_{13}\}$ cores within molecular clusters are scarce. Related notable crystal structures deposited in the Cambridge Structural Database (v 5.37) are a $Pt@Pt_{12}$ cuboctahedron that is edge-bridged by two extra Pt atoms and stabilized by carbonyl and phosphine ligands[14] and a $Ag@Ag_{12}$ cuboctahedron where each triangular face is capped by one iron tetracarbonyl unit.[15]

We have previously demonstrated that hydrides in copper clusters stabilized by dichalcogenolates are substantially hydridic in nature.[6d] Thus terminal alkynes are sufficiently acidic to react with $[Cu_{28}H_{15}(dtc)_{12}]^+$ (dtc = dibutyldithiocarbamate, $S_2CN^nBu_2$) to yield a new NC formulated as $[Cu_{13}(dtc)_6(acetylide)_4]^+$ (**2**; see Scheme 1), which features a centered cuboctahedral $[Cu_{13}]^{11+}$ core with two cluster electrons.

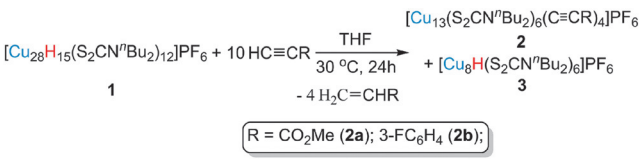

Scheme 1. Synthesis of compounds **2a**, **2b**, and **3**.

A tenfold excess of methyl propiolate was added to a THF suspension of $[Cu_{28}H_{15}(S_2CN^nBu_2)_{12}]^+$, and the reaction mixture was stirred at 30 °C for 24 hours. The color of the suspension changed from orange to deep red, and a dark green solid deposited from the solution. Workup of this mixture led to the isolation of $[Cu_{13}\{S_2CN^nBu_2\}_6\{C{\equiv}CC(O)OMe\}_4](PF_6)$ (**2a**) as a dark red solid in 73% yield. Presumably, the hydrogen generated in situ during the reaction was used to partially reduce the excess alkyne (4 of the 10 equiv of alkyne were reduced to the alkene; see the Supporting Information, Figure S1) as well as some Cu^I species to Cu^0. $[Cu_{13}\{S_2CN^nBu_2\}_6\{3\text{-}FC_6H_4C{\equiv}C\}_4](PF_6)$ (**2b**, 49% yield) was formed under similar reaction conditions by replacing methyl propiolate with $3\text{-}FC_6H_4C{\equiv}CH$. In both cases, **3** was isolated as a side product in 10–15% yield. **2a** and **2b** were fully characterized by single-crystal X-ray diffraction and a broad set of standard chemical characterization methods, including multinuclear NMR spectroscopy, ESI mass spectrometry, and X-ray photoelectron spectroscopy (XPS). The positive-ion ESI mass spectra of **2a** and **2b** clearly display prominent peaks for the molecular ions $[\mathbf{2a}]^+$ and $[\mathbf{2b}]^+$ at *m/z* 2382.8 (calcd 2382.6) and *m/z* 2526.7 (calcd 2526.7), respectively, and their simulated isotopic patterns are in good agreement with the experimentally observed ones (Figures S2 and S3). Most importantly, with one PF_6^- counterion, six dtc, and four alkynyl anionic ligands, the formal global oxidation state of the 13-atom metal core should be +11. Compounds **2** thus are mixed-valent complexes and, more precisely, two-electron superatoms. Notably, only three two-electron NCs are known, namely $[Cu_{25}H_{22}(PPh_3)_{12}]^+$,[8] $[Ag_{14}(SC_6H_3F_2)_{12}(PPh_3)_8]$,[16] and $[Ag_{16}(SC_6H_3F_2)_{14}(dppe)_8]$ (dppe = 1,2-bis(diphenylphosphino)ethane).[17]

The single-crystal X-ray structures of **2a** (Figure 1) and **2b** (Figure S4) clearly show the $Cu@Cu_{12}$ cuboctahedral architecture of the cations.[18] To the best of our knowledge, this core unit is the first example of a copper-centered Cu_{13} cuboctahedron, identical to that observed in the fcc structure of bulk copper. This configuration represents a marked contrast to the centered icosahedral geometry observed in the core units of $[Ag_{20}\{S_2P(O^nPr)_2\}_{12}]$, $[Ag_{21}\{S_2P(O^iPr)_2\}_{12}]^+$, and $[Au_{13}(PPhMe_2)_{10}Cl_2]^{3+}$.[5,19] The central copper atom (Cu1) acts a template in the formation of this large cluster, and strongly binds to the twelve other Cu atoms. Whereas a couple of examples of Au_{12} and Ag_{12} dodecahedra that encapsulate a sodium or silver atom, respectively, are known,[14,20] **2** is the first example of a copper cuboctahedron encapsulating another atom. It is noteworthy that no guest element is present in the dodecahedral structures of $[Cu_{12}S_8]^{4-}$,[21a] $[Cu_{12}(NPh)_8]^{4-}$,[21b] $[(^tBu_3SiP)_6Cu_{12}]$,[21c] and $[Cu_{12}E_6(PR_3)_8]$ (E = S, Se, Te).[21d] The six square faces of the cuboctahedron in **2** are all capped by six dtc ligands that bridge four metal centers in a μ_2,μ_2 binding mode. The twelve sulfur atoms thus form a truncated tetrahedral cage. Only half of the eight triangular faces of the cuboctahedron are capped by alkynyl groups in a μ_3-η^1 fashion. Each of the twelve outer Cu atoms is tricoordinated to two S atoms and one C atom in a somewhat pyramidalized trigonal arrangement (**2a**: S1-Cu2-C55 117.7(5)°, S1-Cu2-S3 105.8(2)°). As a result, **2** has an idealized T_d symmetry.

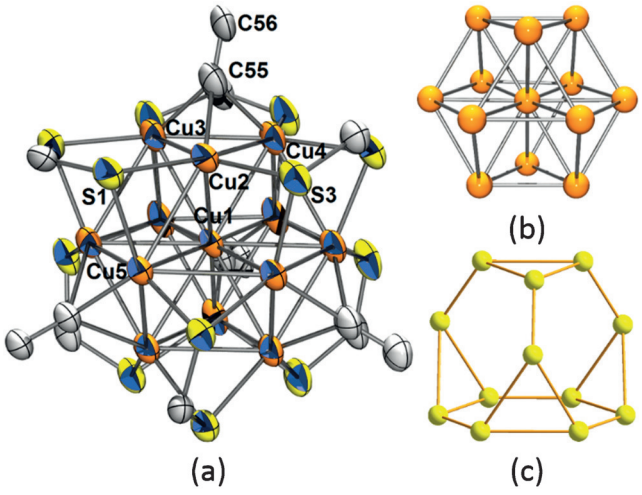

Figure 1. a) Structure of the cluster cation of **2a**. Thermal ellipsoids set at 30% thermal probability. All N^nBu_2 and $C(O)OCH_3$ moieties were omitted for clarity. b) The centered cuboctahedron framework of 13 copper atoms. c) The 12 sulfur atoms with truncated tetrahedral geometry that surround the copper core.

A cuboctahedral configuration of twelve metal atoms around the central μ_{12}-Cu atom in **2** generates a geometric entity derived from the fcc packing of elemental copper. The Cu–Cu distances in **2a** and **2b** range from 2.522(4) to 2.786(3) Å and from 2.484(1) to 2.792(2) Å, respectively, and are shorter than the average Cu–Cu distance (2.845 Å) observed in cuboctahedral $[Cu_{12}S_8]^{4-}$.[21a] The average Cu_{cent}–Cu_{cubo} bond length [2.636(3) Å (**2a**), 2.645(2) Å (**2b**)] is comparable to that of the Cu_{cent}–Cu_{icos} bond (2.635 Å) in $[Cu_{25}H_{22}(PPh_3)_{12}]Cl$ and about 0.1 Å longer than that in metallic copper.[22] Although $[Cu_{20}H_{11}\{Se_2P(O^iPr)_2\}_9]$ also consists of a distorted cuboctahedral Cu_{13} core with the central copper atom further linked to a hydride, the Cu–Cu distances are in the range of 2.5051(4)–3.0911(6) Å.[6f] The Cu–S bond lengths, averaging 2.289(6) Å in **2a** and 2.299(3) Å in **2b**, are comparable to the average Cu–S distances in $[Cu_8(H)(S_2CN^nPr_2)_6]^+$ (2.314(2) Å) with a similar ligand S···S bite distance of 3.044 Å.[6a] The average Cu–C bond lengths [2.035(2) Å (**2a**), 2.039(1) Å (**2b**)] are less than the sum of the covalent radii for σ-bonded alkynes.[23] The four C≡C–C angles of the four acetylide ligands in **2a** deviate from linearity by 3°, 9°, 10°, and 16°, respectively, whereas in the case of **2b**, the deviations only amount to 4°, 5°, 8°, and 8°. Similar bonding modes of acetylide ligands have also been observed in other trinuclear copper(I) acetylide complexes.[23] The cluster shows significant distortions away from the idealized T_d symmetry, which could arise from the different electronic and steric requirements of the alkynyl and dtc ligands.

XPS analysis has been used to evaluate the chemical states of metal cores in nanomaterial studies. In the Cu 2p region, the spectrum shows two peaks that are identical for **2a** and **2b** at 932.0 and 952.0 eV (Figures 2 and S5), which were assigned to the $2p_{3/2}$ and $2p_{1/2}$ features of Cu^0. The binding energy (BE) of Cu^I $2p_{3/2}$ in Cu_2O is 932.1 eV.[24] Thus the BE values are

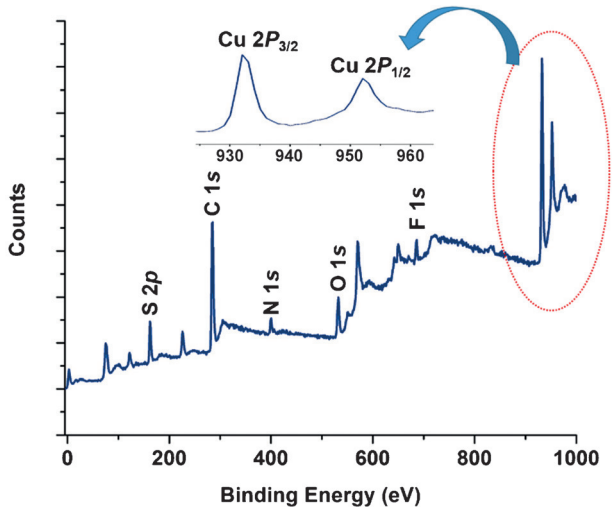

Figure 2. XPS survey spectrum of cluster **2a**, confirming the presence of Cu, S, C, N, F, and O. The inset shows the expanded XPS spectrum in the Cu 2p region of cluster **2a**. Sharp peaks with narrow widths were observed.

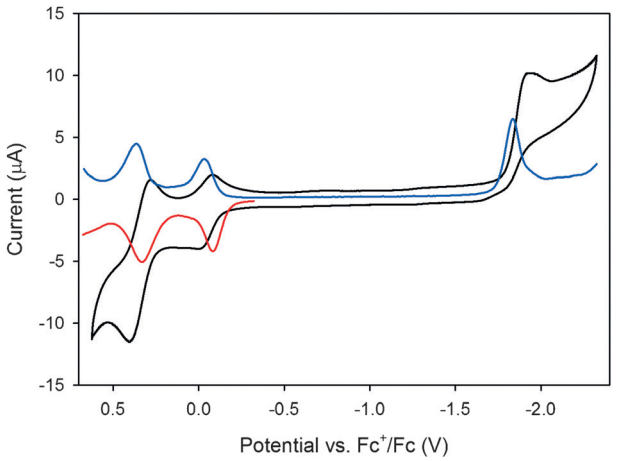

Figure 3. Cyclic voltammogram (black) and differential pulse voltammograms (anodic scan in blue and cathodic scan in red; amplitude: 50 mV, pulse period: 0.5 s, pulse width: 50 ms) of **2a** (0.75 mM) at 273 K in CH_2Cl_2 under N_2 atmosphere (3 mm vitreous carbon electrode, 0.1 M $[^nBu_4N][B(C_6F_5)_4]$).

within the range expected for Cu^0 and Cu^I. The XPS features of all other elements were found to be exactly as expected. The results strongly confirmed the presence of N and O, as demonstrated by the N 1s peak at 400.0 eV and the O 1s peak at 532.0 eV. The S 2p region shows a $2p_{3/2}$ feature at 162.0 eV, which is characteristic of thiolates, and the C 1s peak was located at 285.0 eV, characteristic of the ligand chain.

The ^1H and ^{13}C NMR spectra show one set of resonances, illustrating that the molecule is symmetric in solution (Figures S6–S9). The FTIR spectra of **2a** and **2b** (Figures S10 and S11) show that the ν(C≡C) stretching vibrations of the coordinated RC≡C$^-$ ligands are found at lower frequencies than those of the free ligands (ν(HC≡CC(O)OMe) = 2129, ν(HC≡CC$_6$H$_4$F) = 2107 cm^{-1}). **2a** and **2b** show bands at 2017.5 and 2009.1 cm^{-1}, respectively. These values are slightly higher than that for $[Cu_3(\mu\text{-dppm})_3(\mu_3\text{-}\eta^1\text{-C}{\equiv}\text{CCOO})(\mu_3\text{-OCH}_3)]$ (1976 cm^{-1}).[25] The UV/Vis spectrum of **2a** shows broad multiband optical absorption bands (at 345, 506, 526, and 556 nm) and an intense absorption band at 287 nm (Figure S12), whereas the same number of absorption bands but with shifted positions (304, 335, 510, 539, and 568 nm) were observed for **2b** (Figure S13). The low-energy bands could be assigned by TDDFT calculations to the HOMO–LUMO transition, which corresponds to a metal to ligand charge transfer (MMLCT, see below and Figure S14). Compounds **2a** and **2b** are not emissive in both the solid state and in solution under UV irradiation even at 77 K.

The electrochemical properties of **2a** and **2b** were investigated in CH_2Cl_2 solution at various temperatures. Cyclic voltammograms (CVs) of **2a** obtained at 273 K displayed an irreversible reduction process at $E_{pc} = -1.94$ V (vs. Fc^+/Fc) and two quasi-reversible oxidation events at $E_{1/2} = -0.05$ and $+0.34$ V (Figure 3). At 237 K, the reversibility of all redox waves was slightly improved (Figure S15). Every redox reduction was a one-electron event according to differential pulse voltammetry. The two oxidation peaks, which correspond to the $[Cu_{13}]^{12+}$ and $[Cu_{13}]^{13+}$ species, respectively (see below), are separated by approximately 400 mV, and structural changes might occur upon oxidation owing to the quasi-reversibility of the waves at low temperatures. A similar behavior was observed for analogue **2b** (Figure S16). The current amplitude for the return cathodic wave of the first oxidation event was enhanced at 243 K at a scan rate of 1.6 V s^{-1}. We suggest that **2a** is more stable than **2b** towards oxidation because the HOMO of **2a** (see below) is stabilized by the stronger electron-withdrawing group on the acetylide.

DFT calculations were carried out at the PBE0/Def2-TZVP level of theory on the simplified model compound $[Cu_{13}(S_2CNH_2)_6(C{\equiv}CH)_4]^+$ (**2′**). Its optimized structure, characterized as an energy minimum (no imaginary frequency), was found to be of T_d symmetry. Its metrics match quite well with the X-ray data of **2a** and **2b** (see Table 1). The shortest Cu–Cu distances correspond to the edges of the triangular faces capped by the alkynyl ligands (2.595 Å) and the largest ones to those of the uncapped triangular faces (2.725 Å). On average, the dodecahedral edges are equal to the Cu_{cent}–

Table 1: Selected bond lengths [Å] and angles [°] for **2a**, **2b**, and **2′**.

	2a	**2b**	**2′** (T_d)
Cu_{cent}–Cu_{cubo}	2.605(3)–2.669(3) avg. 2.636(3)	2.601(2)–2.666(2) avg. 2.645(2)	2.660
Cu_{cubo}–Cu_{cubo}	2.522(4)–2.786(3) avg. 2.636(3)	2.484(1)–2.792(2) avg. 2.645(2)	2.595–2.725 avg. 2.660
Cu_{cubo}–S	2.257(6)–2.320(6) avg 2.289(6)	2.338(2)–2.268(3) avg. 2.299(3)	2.344
Cu_{cubo}–C	2.001(2)–2.076(2) avg 2.035(2)	1.977(1)–2.092(1) avg. 2.039(1)	2.053
C≡C	1.187(19)–1.213(7) avg 1.202(12)	1.201(2)–1.231(1) avg. 1.216(15)	1.221
Cu3-Cu2-Cu4	61.13(9)	59.67(6)	60
Cu3-Cu2-Cu5	88.63(9)	87.07(5)	90
C55≡C56-C57	177(2)	175(2)	180

Cu_{cubo} distances (2.660 Å). The electronic structure of **2′** is fully consistent with that of a two-electron superatom. Its Kohn–Sham MO diagram (Figure 4) exhibits a substantial energy gap of 3.08 eV separating the a_1 HOMO, which can be identified as the 1S jellium orbital, from the t_2 lowest

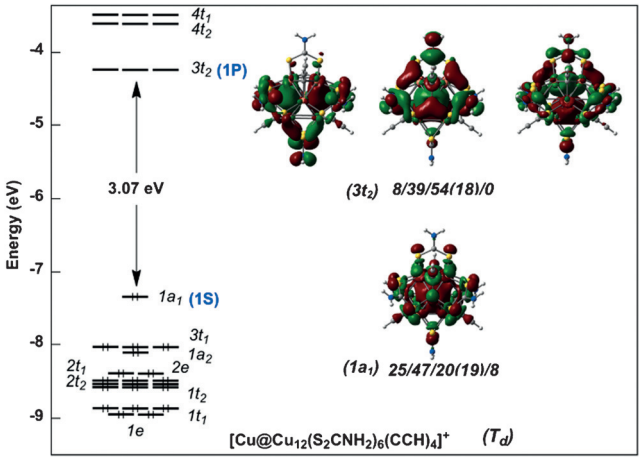

Figure 4. MO diagram of the **2′** model compound. The MO localization (in %) is given as follows: (μ_{12}-Cu)/Cu_{12}/(S_2CNH_2) (of which S)/C≡CH.

unoccupied level, which can be viewed as the 1P jellium shell, mixed with ligand dtc π* orbitals. The metal natural atomic orbital (NAO) charges are −0.54 and +0.69 for Cu_{cent} and Cu_{cubo}, respectively. This corresponds to NAO configurations of $4s^{1.52}3d^{9.93}4p^{0.08}5s^{0.01}$ (Cu_{cent}) and $4s^{0.41}3d^{9.85}4p^{0.04}5s^{0.01}$ (Cu_{cubo}). This is consistent with the view of a formal Cu^{1-} atom at the center interacting with a $[Cu_{12}(S_2CNH_2)_6(C{\equiv}CH)_4]^{2+}$ cage. The twelve pyramidalized Cu^{I} centers of this cage are highly unsaturated, in such a way that each of them bears a vacant sp-type orbital pointing towards the center of the cage. Owing to significant orbital overlap, the twelve sp-type combinations split in energy. The lowest one is a fully in-phase a_1 combination. This accepting orbital is well suited for interacting strongly with the 4s occupied orbital of the encapsulated Cu^{1-} atom, giving rise to the bonding a_1 HOMO of **2′** (Figure 4). This HOMO contains the two electrons associated with the jellium $1S^2$ configuration. On the other hand, the next bonding sp-type vacant combination of the twelve Cu^{I} centers is of t_2 symmetry and matches with the vacant high-lying 4p orbitals of the encapsulated Cu^{1-} center; the resulting bonding combination is the t_2 LUMO of **2′**, which can be viewed as the unoccupied jellium 1P level (with substantial ligand admixture). The computed Cu–Cu Wiberg indices are consistent with the existence of two bonding jellium electrons: +0.060 (Cu_{cent}–Cu_{cubo}) and +0.048 (avg. Cu_{cubo}–Cu_{cubo}). Based on the above analysis, we anticipate that the $[Cu_{12}(dtc)_6(C{\equiv}CR)_4]^{2+}$ cage might be able to host various types of anions, not only two-electron anions isolobal to Cu^{1-}, but also eight-electron anions such as halides or chalcogenides that have occupied valence orbitals perfectly suited for matching the a_1 and t_2 accepting orbitals of the cage.

The oxidized forms of **2′**, namely $[Cu_{13}(S_2CNH_2)_6(C{\equiv}CH)_4]^{n+}$ ($n=2$, 3), were also calculated at the same level of theory. They correspond to the progressive depopulation of the Cu_{13}-centered $1a_1$ HOMO of **2′**. Consistently, their optimized structures (characterized as true energy minima) retain the T_d symmetry, with the metal core expansion increasing with n (Cu_{cent}–Cu_{cubo} = 2.734 and 2.818 Å for $n=$ 2 and 3, respectively). These results are fully consistent with the CV experiments. The computed first and second ionization energies of **2′** are 8.06 and 10.84 eV, respectively.

In summary, we have isolated and fully characterized $[Cu_{13}(alkynyl)_4(dtc)_6](PF_6)$ (**2**), the first centered cuboctahedral copper NCs, which can be considered as models of the bulk copper fcc structure, with partial Cu^0 character. The Cu_{13} skeleton is capped by acetylide groups on four of the eight triangular faces, and each of the six square faces of the cuboctahedron is bridged by a dithiocarbamate ligand. As a result, compound **2** has an idealized T_d symmetry. DFT calculations are fully consistent with the description of these species as two-electron superatoms. Cyclic voltammetry experiments and DFT calculations suggest that the isolation of both $[Cu_{13}]^{12+}$ and $[Cu_{13}]^{13+}$ species should now be possible. It is now clear that **1** could be a good source for larger Cu NCs with partial Cu^0 character. Furthermore, the unique reactivity of **1** should enable the development of reduction reactions of alkynes and various carbonyl derivatives, including unsaturated ketones, esters, and aldehydes. Such work is in progress.

Acknowledgements

This work was supported by the Ministry of Science and Technology in Taiwan (MOST 103-2113-M-259-003). The GENCI-CINES and GENCI-IDRISS French national computer centers are acknowledged for providing computational resources (x2016-087367).

Keywords: centered cuboctahedra · copper · nanoclusters · superatoms · X-ray diffraction

How to cite: *Angew. Chem. Int. Ed.* **2016**, *55*, 14704–14708
Angew. Chem. **2016**, *128*, 14924–14928

[1] a) H. Hakkinen, *Chem. Soc. Rev.* **2008**, *37*, 1847–1859; b) G. Schmid, *Chem. Soc. Rev.* **2008**, *37*, 1909–1930; c) S. Yamazoe, K. Koyasu, T. Tsukuda, *Acc. Chem. Res.* **2014**, *47*, 816–824; d) G. Li, R. Jin, *Acc. Chem. Res.* **2013**, *46*, 1749–1758.

[2] a) M.-C. Daniel, D. Astruc, *Chem. Rev.* **2004**, *104*, 293–346; b) J. F. Parker, C. A. Fields-Zinna, R. W. Murray, *Acc. Chem. Res.* **2010**, *43*, 1289–1296; c) K. M. Harkness, Y. Tang, A. Dass, J. Pan, N. Kothalawala, V. J. Reddy, D. E. Cliffel, B. Demeler, F. Stellacci, O. M. Bakr, J. A. McLean, *Nanoscale* **2012**, *4*, 4269–4274.

[3] a) M.-E. Moret, L. Zhang, J. C. Peters, *J. Am. Chem. Soc.* **2013**, *135*, 3792–3795; b) D. S. Weinberger, N. Amin Sk, K. C. Mondal, M. Melaimi, G. Bertrand, A. C. Stückl, H. W. Roesky, B. Dittrich, S. Demeshko, B. Schwederski, W. Kaim, P. Jerabek, G. Frenking, *J. Am. Chem. Soc.* **2014**, *136*, 6235–6238.

[4] a) P. Jerabek, H. W. Roesky, G. Bertrand, G. Frenking, *J. Am. Chem. Soc.* **2014**, *136*, 17123–17135; b) C. Ganesamoorthy, J. Weßing, C. Kroll, R. W. Seidel, C. Gemel, R. A. Fischer, *Angew. Chem. Int. Ed.* **2014**, *53*, 7943–7947; *Angew. Chem.* **2014**, *126*, 8077–8081.

[5] a) R. S. Dhayal, J.-H. Liao, Y.-C. Liu, M.-H. Chiang, S. Kahlal, J.-Y. Saillard, C. W. Liu, *Angew. Chem. Int. Ed.* **2015**, *54*, 3702 – 3706; *Angew. Chem.* **2015**, *127*, 3773 – 3777; b) R. S. Dhayal, Y.-R. Lin, J.-H. Liao, Y.-J. Chen, Y.-C. Liu, M.-H. Chiang, S. Kahlal, J.-Y. Saillard, C. W. Liu, *Chem. Eur. J.* **2016**, *22*, 9943 – 9947.

[6] a) P.-K. Liao, C.-S. Fang, A. J. Edwards, S. Kahlal, J.-Y. Saillard, C. W. Liu, *Inorg. Chem.* **2012**, *51*, 6577 – 6591; b) R. S. Dhayal, J.-H. Liao, Y.-R. Lin, P.-K. Liao, S. Kahlal, J.-Y. Saillard, C. W. Liu, *J. Am. Chem. Soc.* **2013**, *135*, 4704 – 4707; c) J.-H. Liao, R. S. Dhayal, X. Wang, S. Kahlal, J.-Y. Saillard, C. W. Liu, *Inorg. Chem.* **2014**, *53*, 11140 – 11145; d) A. J. Edwards, R. S. Dhayal, P.-K. Liao, J.-H. Liao, M.-H. Chiang, R. O. Piltz, S. Kahlal, J.-Y. Saillard, C. W. Liu, *Angew. Chem. Int. Ed.* **2014**, *53*, 7214 – 7218; *Angew. Chem.* **2014**, *126*, 7342 – 7346; e) R. S. Dhayal, J.-H. Liao, S. Kahlal, X. Wang, Y.-C. Liu, M.-H. Chiang, W. E. van Zyl, J.-Y. Saillard, C. W. Liu, *Chem. Eur. J.* **2015**, *21*, 8369 – 8674; f) R. S. Dhayal, J.-H. Liao, X. Wang, Y.-C. Liu, M.-H. Chiang, S. Kahlal, J.-Y. Saillard, C. W. Liu, *Angew. Chem. Int. Ed.* **2015**, *54*, 13604 – 13608; *Angew. Chem.* **2015**, *127*, 13808 – 13812; g) R. S. Dhayal, W. E. van Zyl, C. W. Liu, *Acc. Chem. Res.* **2016**, *49*, 86 – 95.

[7] S. G. Bratsch, *J. Phys. Chem. Ref. Data* **1989**, *18*, 1 – 21.

[8] a) T.-A. D. Nguyen, Z. R. Jones, B. R. Goldsmith, W. R. Buratto, G. Wu, S. L. Scott, T. W. Hayton, *J. Am. Chem. Soc.* **2015**, *137*, 13319 – 13324; b) K. Freitag, H. Banh, C. Gemel, R. W. Seidel, S. Kahlal, J.-Y. Saillard, R. A. Fischer, *Chem. Commun.* **2014**, *50*, 8681 – 8684; c) H. Yang, Y. Wang, J. Yan, X. Chen, X. Zhang, H. Hakkinen, N. Zheng, *J. Am. Chem. Soc.* **2014**, *136*, 7197 – 7200.

[9] The structure of $[H_3Rh_{13}(CO)_{24}]^{2-}$ is anticuboctahedral and related to the hcp lattice; see: V. G. Albano, A. Ceriotti, P. Chini, G. Ciani, S. Martinengo, W. M. Anker, *J. Chem. Soc. Chem. Commun.* **1975**, 859 – 860.

[10] C. Zeng, R. Jin, *Struct. Bonding (Berlin)* **2014**, *161*, 87 – 116.

[11] C. Zeng, H. Qian, T. Li, G. Li, N. L. Rosi, B. Yoon, R. N. Barnett, R. L. Whetten, U. Landman, R. Jin, *Angew. Chem. Int. Ed.* **2012**, *51*, 13114 – 13118; *Angew. Chem.* **2012**, *124*, 13291 – 13295.

[12] C. Zeng, T. Li, A. Das, N. L. Rosi, R. Jin, *J. Am. Chem. Soc.* **2013**, *135*, 10011 – 10013.

[13] C. L. Cleveland, U. Landman, T. G. Schaaff, M. N. Shafigullin, P. W. Stephens, R. L. Whetten, *Phys. Rev. Lett.* **1997**, *79*, 1873 – 1876.

[14] J. A. K. Howard, J. L. Spencer, D. G. Turner, *J. Chem. Soc. Dalton Trans.* **1987**, 259 – 262.

[15] a) V. G. Albano, L. Grossi, G. Longoni, M. Monari, S. Mulley, A. Sironi, *J. Am. Chem. Soc.* **1992**, *114*, 5708 – 5713; b) V. G. Albano, F. Calderoni, M. C. Iapalucci, G. Longoni, M. Monari, P. Zanello, *J. Cluster Sci.* **1995**, *6*, 107 – 123; c) D. Collini, C. Femoni, M. C. Iapalucci, G. Longoni, *C. R. Chim.* **2005**, *8*, 1645 – 1654.

[16] L. Gell, L. Lehtovaara, H. Häkkinen, *J. Phys. Chem. A* **2014**, *118*, 8351 – 8355.

[17] a) H. Yang, J. Lei, B. Wu, Y. Wang, M. Zhou, A. Xia, L. Zheng, N. Zheng, *Chem. Commun.* **2013**, *49*, 300 – 302; b) H. Yang, Y. Wang, N. Zheng, *Nanoscale* **2013**, *5*, 2674 – 2677.

[18] CCDC 1501795 (**2a**) and 1501796 (**2b**) contain the supplementary crystallographic data for this paper. These data can be obtained free of charge from The Cambridge Crystallographic Data Centre.

[19] C. E. Briant, B. R. C. Theobald, J. W. White, L. K. Bell, D. M. P. Mingos, A. J. Welch, *J. Chem. Soc. Chem. Commun.* **1981**, 201 – 202.

[20] S.-P. Huang, M. G. Kanatzidis, *Angew. Chem. Int. Ed. Engl.* **1992**, *31*, 787 – 789; *Angew. Chem.* **1992**, *104*, 799 – 801.

[21] a) P. Betz, B. Krebs, G. Henkel, *Angew. Chem. Int. Ed. Engl.* **1984**, *23*, 311 – 312; *Angew. Chem.* **1984**, *96*, 293 – 294; b) P. Reiß, D. Fenske, *Z. Anorg. Allg. Chem.* **2000**, *626*, 1317 – 1331; c) N. Wiberg, A. Wörner, D. Fenske, H. Nöth, J. Knizek, K. Polborn, *Angew. Chem. Int. Ed.* **2000**, *39*, 1838 – 1842; *Angew. Chem.* **2000**, *112*, 1908 – 1912; d) O. Fuhr, S. Dehnen, D. Fenske, *Chem. Soc. Rev.* **2013**, *42*, 1871 – 1906, and references therein.

[22] J. A. Goedkoop, A. F. Andresen, *Acta Crystallogr.* **1955**, *8*, 118 – 119.

[23] A. Makarem, R. Berg, F. Rominger, B. F. Straub, *Angew. Chem. Int. Ed.* **2015**, *54*, 7431 – 7435; *Angew. Chem.* **2015**, *127*, 7539 – 7543.

[24] a) Z. Ai, L. Zhang, S. Lee, W. Ho, *J. Phys. Chem. C* **2009**, *113*, 20896 – 20902; b) T. Ghodselahi, M. A. Vesaghi, A. Shafiekhani, A. Baghizadeh, M. Lameii, *Appl. Surf. Sci.* **2008**, *255*, 2730 – 2734.

[25] H.-Y. Chao, L. Wu, B.-C. Su, X.-L. Feng, *Inorg. Chem. Commun.* **2011**, *14*, 122 – 124.

Received: September 2, 2016
Published online: October 26, 2016

